

# Fabrication of PLGA Conduit for Peripheral Nerve Regeneration

Nastaran Doubra<sup>1,2</sup>, Afsaneh Amiri<sup>2</sup>, Masoumeh Foroutan koudehi<sup>1,2</sup>, Zahra Jamalpoor<sup>4</sup>, Abbas Ali Imani Fooladi<sup>3</sup>, Nourani Mohammad Reza<sup>1\*</sup>

*1.Division of Tissue Engineering, Applied Biotechnology Research Center, Baqiyatallah University of Medical Sciences, Tehran, Iran*

*2.Department of Chemistry, Islamic Azad University, Central Tehran Branch, Tehran, Iran*

*3.Applied Microbiology Research Center, Baqiyatallah University of Medical Sciences, Tehran, Iran, Tehran, Iran*

*4. Tissue Engineering Department, cellular and molecular research center of Iran University of Medical Sciences, Tehran, Iran*

Received: 23 July 2013 / Accepted: 4 December 2013

## Abstract

PLGA conduits are widely used experimentally as scaffold for the reconstruction of damaged peripheral nerves. But post traumatic and post operation infections are the most common complications. Silver nanoparticles, as potent antimicrobial agent, have diverse medical applications ranging from silver based wound dressings to silver coated implants. In this study, we fabricated and characterized PLGA/Nanosilver scaffolds for peripheral nerve regeneration and evaluated their antibacterial and cytotoxicity behavior. The results showed that antibacterial efficacy increases with the increase in concentration of silver nanoparticle. This work suggests that nanosilver coating of PLGA scaffolds can increase their infection resistancy and potentially improve peripheral nerve regeneration in a dose dependent manner.

**Key Words:** PLGA, Nanosilver, Nerve Growth Conduit, Peripheral Nerve Regeneration

## Introduction

Peripheral nerve defects are as a result of trauma, pathology, surgery, or various diseases that couldn't be recovered through normal bodily repair processes and result in loss of normal neurologic function [1,2]. Peripheral nerve injury can successfully heal, if an appropriate environment and route be provided [3]. This condition requires the use of nerve grafts and peripheral nerve substitutes to support the healing process. Autografts have been considered as the gold standard for nerve grafts due to their brilliant properties; however there are restrictions on autografts use such as limitations in availability of donor site, formation of neuroma and donor site morbidity. Allografts, on the other hand, are relatively plentiful in source, but yet have the potential risk of pathogen transmission and are thus lower in value

promotion of nerve regeneration as compared to autografts. An emerging contemporary strategy to surmount these complications are a variety of nerve graft substitutes, as nerve growth conduits structurally based on ceramics and polymers [4, 5, 6]. Conduits of different composition have been developed to improve nerve gap regeneration [7]. Artificial biodegradable polymers are attractive candidates for scaffold fabrication because they don't carry the risk of disease transmission and immunorejection. They degrade and resorb after nerve restoration, thus removing the long-term inflammation and complications associated with foreign body reactions [8, 9, 10,11]. Among biocompatible and biodegradable biomaterials, Poly (lactic-co-glycolic acid) (PLGA) has necessary characterization. PLGA has been the most frequently used biodegradable polymer in tissue engineering for fabricating porous foams for biomedical applications. This is a necessary polymer

\*Corresponding Authors: Nourani Mohammad Reza  
Tehran, Iran. Tel/Fax: 98-21-88211523, r.nourani@yahoo.com

because it degrades into lactic and glycolic acid, moderately harmless to the growing cells. Its mechanical and degradation properties can be finely tuned through variations in molecular weight and copolymer ratio to give degradation times from months to several years [12, 13, 14]. Post traumatic infection in peripheral nerve injury should be prevented using antibacterial agents, for which nanosilver particles are a suitable candidate.

Antibiotic overuse led to the development of antibiotic resistant bacteria and therefore silver as antibacterial agent seems to be important [15]. Since long time ago, metallic silver and its salts (e.g., silver nitrate) has been used to treat wounds, abscesses and fistulas [16, 17]. Silver in the form of nanoparticles is quite an effective antimicrobial substrate and is used in different health care materials such as wound dressings [18, 19]. Silver nanoparticles (Ag Ns) exert their antibacterial activity via interacting with the sulfur containing proteins present in cell membrane and with phosphorus containing DNA as well. Nanosilver also attacks to the bacterial respiratory system, with releasing silver ions inside the cells improving their bactericidal activity [20, 21, 22, 23, 24].

In this work, we aimed to develop PLGA conduits enhanced with nanosilver to connect the two disrupted neural ends and improve peripheral nerve regeneration.

## Materials and Methods

### Fabrication of PLGA Conduit

Initially, a 25% solution of (D,L) polylactide-co-glycolide (PLGA) in a 50:50 monomer ratio (Sigma-Aldrich-Germany) and molecular weight 40000-75000 g/mol was prepared in 1,4-dioxane solvent (Merk-Germany) at 50°C for 5h. Conduits were prepared by dip-coating method. Briefly, special tootings were dipped in PLGA solution and placed in 20% concentration of isopropyl alcohol, as the nonsolvent, at room temperature overnight. The samples were formed as a result of solvent-nonsolvent phase conversion. They were then washed with deionized water repeatedly. Specimens were air-dried and manually demolded from the tootings, after which the samples were freeze dried at -57°C for 32h. The resulting PLGA conduits had the following dimensions: Inter diameter 1.8 mm, Outer diameter 2 mm, thickness 0.1 mm and length about 12 mm.

### Conduit coating with Nanosilver

After PLGA conduit preparation, their surface was coated with nanosilver particles, by soaking into different nanosilver concentrations of colloidal nanosilver solution (Nanocid, Iran) at 25°C for 72h (Table 1). The minimum inhibitory concentration (MIC) and minimum bactericidal concentration (MBC) of nanosilver solution were in the range of 1.95-1000 and 25.62 µg/mL respectively. The conduits were finally air dried

## Characterization study

### Physiochemical evaluation

Colloidal nanosilver solution was characterized using TEM (Philips 120 KV). The PLGA/Nanosilver conduits were characterized using SEM/EDX (Seron Technology CO, AIS 2100) and FT-IR (Jasco-410).

Table 1. % concentration of nanosilver in different solutions

Conduits coating type	Amount of polymer composites (in grams)	Concentration of nanosilver (in µL)	Volume of nanosilver (in mL)	Time(h)	Amount of nanosilver present(in mg)
M1	0.5	0.0009	7	72	0.67
M2	0.5	0.0007	7	72	0.52
M3	0.5	0.0004	7	72	0.29
M4	0.5	0.0002	7	72	0.14

M1: extra heavy coated; M2: Heavy coated; M3: Medium coated; M4: Light coated



Fig. 1. Display of about 12-mm PLGA/ Nanosilver conduits intended to substitute a 10mm nerve gap.

### Biological evaluation

**Antibacterial activity test:** Antibacterial activity of PLGA/Nanosilver conduit was assessed, the details of which had already been described elsewhere (Imani Fouladi et. al, article Methods) [25]. Briefly, after preparation of PLGA/Nanosilver conduit anti bacterial effect was determined with the disk diffusion method on Muller Hinton agar with different type of conduits (M1-M4).

**Biocompatibility test:** Biocompatibility test was done according to our previous study [26]. Based on this method, conduits were soaked in 0.0009 µL of Ag Ns, sterilized by ethylene oxide at 38°C for 8h at 65% relative humidity. After 24h exposure to air, ethylene oxide was removed from conduits by placing them into a standard 24-well-plate and were first washed with sterile distilled water, and then with 0.9% NaCl sterile solution and finally with culture

medium. Then, Dulbecco's Modified Eagle Medium (DMEM) cell culture media containing 1% (v/v) penicillin/streptomycin (PS) and 10% (v/v) fetal bovine serum (FBS) were used. Chinese hamster ovary cells (CHO) with a density of  $4 \times 10^5$  cell/mL were added to the samples in PS plates and maintained in incubator ( $37^\circ\text{C}$ , 5%  $\text{CO}_2$ ) for 48h. The samples were fixed in 100% ethanol for 15min, and then seen by light microscopy (Nikon Eclipse 50i).

#### MTT test

MTT is a simple colorimetric assay to measure cell proliferation and viability (26). This test was performed to assess the cytotoxicity of four different concentrations of nanosilver used in PLGA/Nanosilver conduits. Cytotoxicity effects of conduits were investigated on rat mesenchymal stem cells (rMSC). The cells were plated in 96-well culture plates at  $1.7 \times 10^4$  cell/well. They were cultured in RPMI-1640 supplemented with 10 % FBS and 1% PS in 5%  $\text{CO}_2$  at  $37^\circ\text{C}$ . After 72h, mediums were removed and 100  $\mu\text{L}$  of fresh medium and 13  $\mu\text{L}$  of MTT solution (5  $\mu\text{g/mL}$ , diluted with RPMI 1640 without phenol red) were added to each well. Incubation was allowed for another 4h in dark at  $37^\circ\text{C}$ . Mediums were removed and 100  $\mu\text{L}$  well DMSO (dimethyl sulfoxide, Sigma, Aldrich, Germany) was added to dissolve formazan crystals. Wells were finally read at 570 nm on an ELISA plate reader (Tecan Sunrise TM) and percentage of viability calculated.

The well without conduit was used as a negative control and cell viability was defined as 100% for MTT assay control. Each test was repeated three times.

## Results

### TEM studies

TEM was used to show the morphology of spherical nanosilver particles. According to the scale bar in fig. 2, it is estimated that the average size of silver nanoparticles was 5.5nm in diameter.

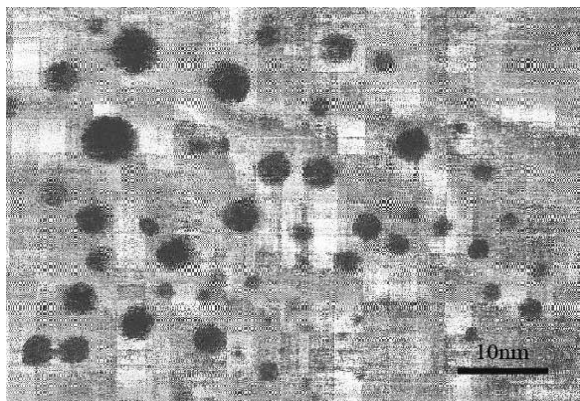


Fig. 2 TEM image of colloidal nanosilver solution shows that the average particle diameter was 5.5 nm.

### SEM studies

SEM was used to assess the surface property of PLGA/Nanosilver conduits. Nanoparticles were not visible at the surface due to their very small spherical size. In addition the outer surface was more porous as compared to the inner surface (Fig. 3)

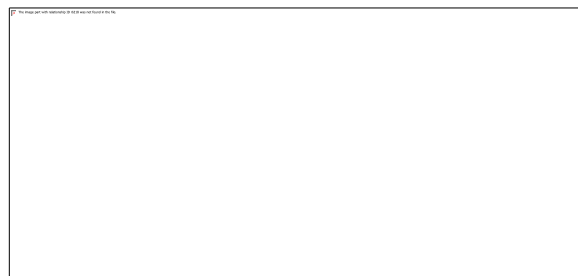


Fig. 3 Cross-sectional, inner and outer surface images of PLGA conduit coated with nanosilver particle taken by SEM.

### EDX Analysis

Figure 4 shows the amount of energy for each element available in the conduit. It indicates that Ag is the minor element. Since the concentration of nanosilver is very low, the intensity of its peak has a very short amplitude. Although the distribution of silver nanoparticles at the conduit surface was not graphed by SEM spectrum, X-ray emission in EDX reveals them.

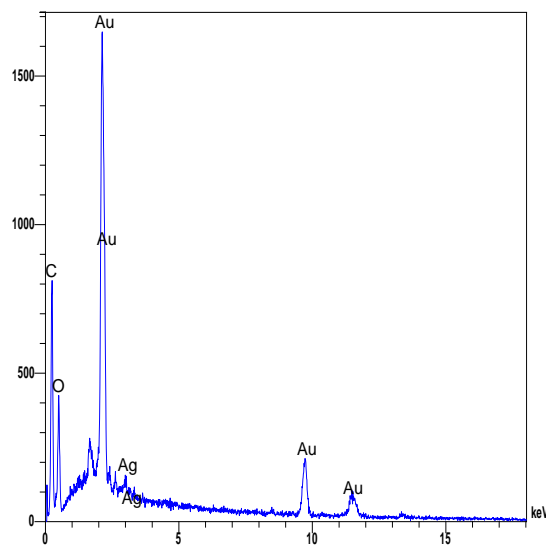


Fig. 4 EDX pattern of PLGA/nanosilver conduits.

According to the map in fig 5, the existence of elements and also distribution of nanosilver particles is achieved in every part of conduit.

### FT-IR spectroscopy

FT-IR spectrum reveals the functional groups in polymer structure in Conduits. The FT-IR spectrum of PLGA (control) and PLGA/Nanosilver neural guidance channels is

shown in fig. 6. There are not specific peak shifts in PLGA/Nanosilver conduits compared to control. Most of

dioxane and isopropyl alcohol have been removed from the conduit during freeze-drying and liquid-liquid demixing process respectively.

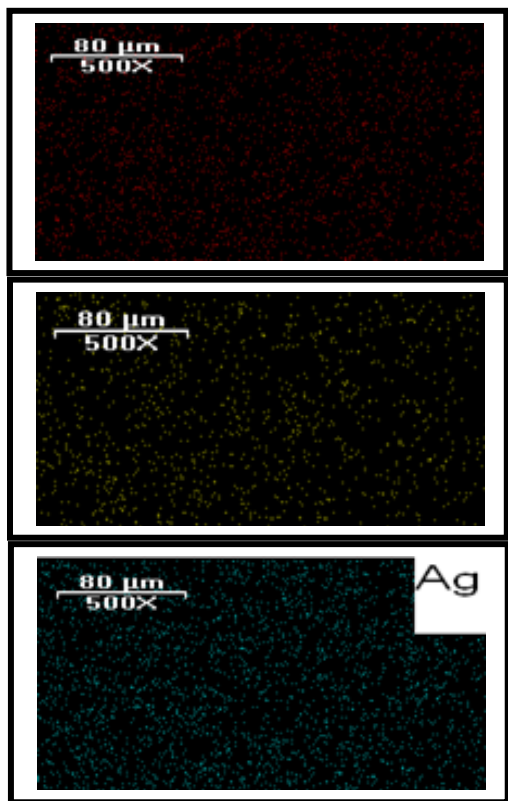


Fig. 5 Map distribution of the elements and distribution of Ag Ns are indicated at the PLGA/Nanosilver conduit surface using EDX analysis

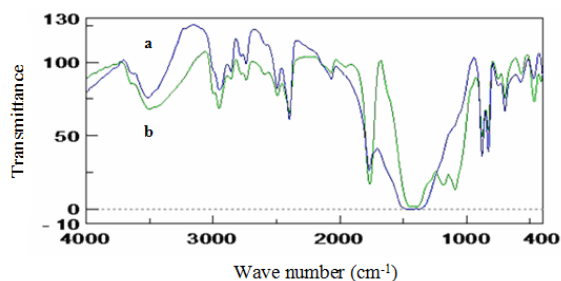


Fig. 6. FT-IR spectroscopy : a (Blue curve) PLGA conduit b (Green curve) PLGA/Nanosilver conduit.

As a result, The bands at  $1100\text{--}1300\text{ cm}^{-1}$  and  $3600\text{--}3650\text{ cm}^{-1}$  corresponded to C-O and O-H respectively, which are assumed to be for the dioxane and isopropyl alcohol existence. However other functional groups such as  $1200\text{ cm}^{-1}$ ,  $1735\text{--}1750\text{ cm}^{-1}$  and  $3000\text{ cm}^{-1}$  were due to C-C, C=O and C-H groups in order, mainly refers to the polymer structure.

## Biological studies

### Antibacterial activity studies

Figure 7A indicates antibacterial activity of PLGA/Nanosilver conduits against gram-negative E.coli while Figure 7B shows the activity against gram positive S.aureus. Inhibition zone around each conduit shows the quality of its activity. When nanosilver concentration is increased, the inhibition zone expanded. As a result their antibacterial activity is for the presence of nanosilver particles on the surface of PLGA conduits and with increasing the nanosilver concentration on the conduit surface this activity was enhanced.

### Biocompatibility test

Since the presence of Dioxane may be toxic, evaluation of cell viability before and after soaking into the  $0.0009\text{ }\mu\text{L}$  of

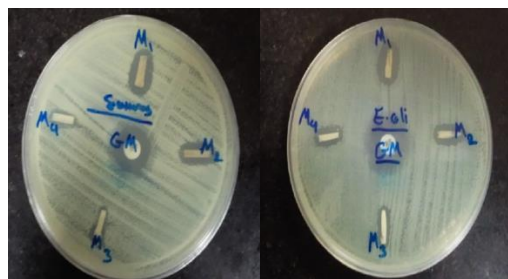


Fig. 7. Antibacterial activity of PLGA/Nanosilver conduits against E.coli (A) and S.aureus (B). The samples were (M1= $0.0009\text{ }\mu\text{L}$ , M2= $0.0007\text{ }\mu\text{L}$ , M3= $0.0004\text{ }\mu\text{L}$ , M4= $0.0002\text{ }\mu\text{L}$ ) and (GM= Gentamycin (10 mg)) control.

nanosilver carried out to make sure of the safety of the conduit. Biocompatibility of both conduits is shown in fig. 8 by cell aggregation growth on the conduits during a 3 day period of incubation.

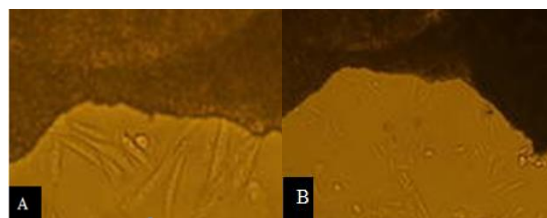


Fig. 8 (CHO) cells cultured on the PLGA conduit (A) and PLGA/Nanosilver conduit (B).

### MTT study

Figure 9 shows results from MTT tests, for four different concentrations of nanosilver. Accordingly, the toxicity increases in direct proportion of nanosilver concentration. Results shows that the bactericidal activity is due to the existence of silver nanoparticles at the PLGA conduit surface.



## Discussion

In this study, we tried to make proper environment for nerve growth by excluding existence of micro-organisms. Although the amount of coated nanosilver at the conduit surface is very low, its bactericidal property provides an opportunity for a better nerve growth the PLGA conduit. TEM micrograph showed that the average size of silver nanoparticles which was too small to be observed via SEM. It might be due to the size of the nanoparticle. According to the report by Madhumathi et al. in developing Chitin/Nanosilver scaffolds for wound dressing application, their particle size was as small as 5nm as such had not been shown in SEM [27]. In the study by Lingzhou Zhao et al. concerning the antibacterial nano-structured titania coating incorporated with silver nanoparticles, TEM image demonstrates that the Ag nanoparticles attached to the inner wall of the titania nanotubes had a diameter of about 10-20nm [28].

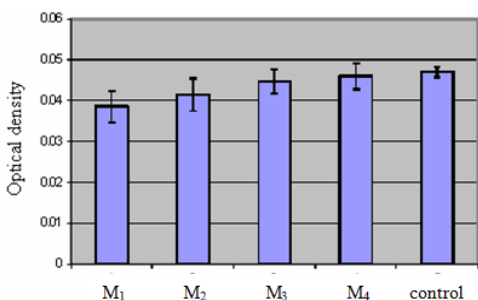


Fig. 9 Biocompatibility of PLGA conduits soaked in different concentrations of nanosilver solution (M<sub>1</sub>=0.0009 $\mu$ L, M<sub>2</sub>=0.0007 $\mu$ L, M<sub>3</sub>=0.0004 $\mu$ L, M<sub>4</sub>=0.0002 $\mu$ L of Ag NS). Once soaked in higher concentration of Ag NS, the number of cells decreased.

According to Shahbazzadeh et al. on a survey of in vitro effects of Nanosilver toxicity on fibroblast and mesenchymal stem cell lines, the morphology of Ag nanoparticles in aquoas solution was obtained by TEM and had an average diameter of 10 nm [29]. By using SEM, pore distribution in the inner and outer surfaces of PLGA/Nanosilver conduit was seen. During dip-coating process, the lumen side was in contact with tooting, whose surface interacted poorly with non-solvent and low porosity of the inner surface was formed. The more porous outer surface, in comparison to the inner surface, may be accounted for by more exposure to isopropyl alcohol. During the immersion of PLGA solution into isopropyl alcohol, due to the phase separation effect, non-solvent influx into the polymer film separates polymer solution into two phases of rich and poor polymer coats and accelerates freezing of the separated structure. Use of deionized water affects liquid-liquid demixing process. Chen-Jung Chang et al. found that the existence of isopropyl alcohol around the polymer coatings can increase the amount of porosities on the conduit surface. They demonstrated that particle size and their percentage can even be altered by changing the volume of non-solvent. They mentioned that the conduit porosities would be increased by increasing the isopropyl alcohol concentration [30]. Fourier Transform Infrared

Spectroscopy (FTIR) didn't show any difference between PLGA and PLGA/Nanosilver conduits. There is probably no chemical reaction between PLGA and nanosilver particles; if so, only a physical adsorption of silver nanoparticle on PLGA conduit is imaginable. The lack of specific peak shifts in FTIR spectrum may be attributed to the absence of any chemical bounds whatsoever. Kumar et al. in 2010 developed a novel b-Chitin/Nanosilver composite scaffold for wound dressing. In their study, two spectrums of b-Chitin and b-Chitin/Nanosilver were similar implying that the silver nanoparticles are interapped into the scaffold [27]. Sekaran Saravanan et al. prepared a Chitosan/Nano hydroxy apatite/Nanosilver for bone tissue engineering. They enriched the scaffold surface by soaking it into silver nitrate solution. Comparing the FTIR spectra of Chitosan/Nano hydroxy apatite and Chitosan/Nano hydroxyl apatite/Nanosilver scaffolds, they demonstrated that the latter spectrum was shifted by the coordinative interaction between NH<sub>2</sub> groups of the chitosan and silver ions [31]. Distribution of silver nanoparticles at the PLGA/Nanosilver conduit is supported by EDX observation. Yu Tsai and colleagues used silver nanoparticles in carbon nanotube-nafion for chemical sensors and showed their distribution by energy dispersive X-ray spectroscopy. Nanosilver was identified in EDX patterns [32].

According to our biological results, antibacterial activity of PLGA/Nanosilver conduit is increased by soaking PLGA channels into higher concentrations of silver nanoparticles. Our results are consistent with those reported by Kumar et al. [27]. In addition, Lin Li et al. evaluated antibacterial activity of Nanosilver/ PLLA membranes against E.coli and staph and claimed that zone inhibition around Ag/PLLA membrane due to the release of silver nanoparticles from PLLA. Bacterial inhibition zone of Ag/PLLA membranes was clear in comparison with PLLA that was set as control specimen [33]. MTT assay is based on the ability of the living cells for reducing tetrazolium salt to formazan. There was significant loss of cell viability as PLGA conduits soaked into higher and higher concentrations of nanosilver. This may be due to the toxicity of higher concentration of silver particles.

Park and colleagues induced cytotoxicity with silver nanoparticles via Trojan-horse type mechanism, by adding AgNs and performed MTT assay and demonstrated when cells were treated with higher concentrations of AgNs, viability of the cultured cells decreased [34]. In a survey performed by Shahbazzadeh et al. the effect of nanosilver toxicity on fibroblast and mesenchymal stem cell lines was assessed. They also reported that the toxic effect of adding nanosilver on cell viability was increases in parallel with AgNs concentration [29].

## Conclusions

In this investigation, PLGA/Nanosilver conduits were characterized by using SEM, FTIR and TEM. Antibacterial efficiency of these conduits were found against both S.aureus and E.coli and were also evaluated by indirect cytotoxicity test using MTT assay.

## Acknowledgments

The authors appreciate Baqiyatallah University of Medical Sciences, Tehran, Iran for their financial burden to perform this project.

## References

1. Wolford LM. Autogenous nerve graft repair of the trigeminal nerve. *Oral Maxillofac Surg Clin North Am.* 1992; 4: 447-457.
2. Mackinnon SE, Dellon AL. *Surgery of the Peripheral Nerve.* New York: Thieme, 1988; 115-119.
3. Li X, Cai Sh, Liu B, Xu Zh, Dai X, Ma K, Li Sh, Yang L. Characteristics of PLGA-gelatin complex as potential artificial nerve scaffold. *Colloids and Surfaces B: Biointerfaces.* 2007; 57: 198-203.
4. Amilo S, Yanez R, Barrios RH. Nerve regeneration in different types of grafts: experimental study in rabbits. *Microsurgery.* 1995; 16: 621-630.
5. Bertelli JA, Orsal D, Mira JC. Median nerve neurotization by peripheral nerve grafts directly implanted into the spinal cord: anatomical, behavioural and electrophysiological evidences of sensorimotor recovery. *Brain Res.* 1994; 644: 150-159.
6. Nikkiah G, Carvalho GA, Samii M. Nerve transplantation and neurolysis of the brachial plexus after post-traumatic lesions. *Orthopade.* 1997; 26: 612-620.
7. Chang JY, Lin JH, Yao CH, Chen JH, Lai TY, Chen YS. In vivo evaluation of a biodegradable EDC/NHS-cross-linked gelatin peripheral nerve guide conduit material. *Macromol Biosci.* 2007; 7: 500-7.
8. Lu L, Garcia CA, Mikos AG. In vitro degradation of thin poly(DL-lactic-co-glycolic acid) films. *J Biomed Mater Res.* 1999; 46(2): 236-244.
9. Ma PX, Zhang R. Synthetic nano-scale fibrous extracellular matrix. *J Biomed Mater Res.* 1999; 46(1): 60-72.
10. Kim SS, Utsunomiya H, Koski JA, Wu BM, Cima MJ, Sohn J, Mukai K, Griffith LG, Vacanti JP. Survival and function of hepatocytes on a novel three-dimensional synthetic biodegradable polymer scaffold with an intrinsic network of channels. *Ann Surg.* 1998; 228(1): 8-13.
11. Ma PX, Schloo B, Mooney D, Langer R. Development of biomechanical properties and morphogenesis of in vitro tissue engineered cartilage. *J Biomed Mater Res.* 1995; 29(12): 1587-1595.
12. Wake MC, Patrick CW, Mikos AG. Pore morphology effects on the fibrovascular tissue growth in porous polymer substrates. *Cell Transplant.* 1994; 3(4): 339-43.
13. Sharkawy AA. Engineering the tissue which encapsulates subcutaneous implants. II. Plasma-tissue exchange properties. *J Biomed Mater Res.* 1998; 40: 586-97.
14. Frazza EJ, Schmitt EE. A new absorbable suture. *J Biomed Mater Res.* 1971; 1: 43.
15. Gemmell CG, Edwards DI, Frainse APJ. Guidelines for the prophylaxis and treatment of methicillin-resistant *Staphylococcus aureus* (MRSA) infections in the UK. *J Antimicrob Chemother.* 2006; 57: 589-608.
16. Klasen HJ. A historical review of the use of silver in the treatment of burns. II. Renewed interest for silver. *Burns.* 2000; 26: 131-8.
17. Castellano JJ, Shafii SM, Ko Donate FG, Wright TE, Mannari RJ. Comparative evaluation of silver-containing antimicrobial dressings and drugs. *Int Wound J.* 2007; 4: 114-22.
18. Ip M, Lui SL, Poon VKM, Lung I, Burd A. Antimicrobial activities of silver dressings: an in vitro comparison. *J Med Microbiol.* 2006; 55: 59-63.
19. Leaper DL. Silver dressings: their role in wound management. *Int Wound J.* 2006; 3: 282-94.
20. Feng QL, Wu J, Chen GQ, Cui FZ, Kim TN, Kim JO. A mechanistic study of the antibacterial effect of silver ions on *Escherichia coli* and *Staphylococcus aureus*. *J Biomed Mater.* 2000; 52: 662-8.
21. Sondi I, Salopek-Sondi B. Silver nanoparticles as antimicrobial agent: a case study on *E. coli* as a model for Gram-negative bacteria. *J Colloid Interface.* 2007; 275: 177-82.
22. Morones JR, Elechiguerra JL, Camacho A, Ramirez JT. The bactericidal effect of silver nanoparticles. *Nanotechnology.* 2005; 16: 2346-53.
23. Song HY, Ko KK, Oh LH, Lee BT. Fabrication of silver nanoparticles and their antimicrobial mechanisms. *Eur Cells Mater.* 2006; 11: 58.
24. Jain P, Pradeep T. Potential of silver nanoparticle-coated polyurethane foam as an antibacterial water filter. *Biotechnol Bioeng.* 2005; 90: 59-63.
25. Mehrab R, Imani Fooladi AA, Amir Mozafari N, Nourani MR. A Study on the Antibacterial Activity of Nanosilver Colloidal Solution against ESBL-Producing *Pseudomonas aeruginosa*. *Current Nanoscience.* 2012; 8(5): 1-5.
26. Hafezi F, Hosseinnajad F, Imani Fooladi AA, Mohit Mafi S, Amiri A, Nourani MR. Transplantation of nano-bioglass/gelatin scaffold in a non-autogenous setting for bone regeneration in a rabbit ulna. *J Mater Sci Mater Med.* 2012; DOI: 10.1007/s10856-012-4722-3
27. Kumar PT, Abhilash S, Manzoor K, Nair SV, Tamura H, Jayakumar R. Preparation and characterization of novel b-chitin/nanosilver composite scaffolds for wound dressing applications. *Carbohydrate Polymers.* 2010; 80: 761-767
28. Wang H, Huo K, Cui L, Zhang W, Ni H, Zhang Y, Wu Z, Chu PK. Antibacterial nano-structured titania coating incorporated with silver nanoparticles. *Biomaterials.* 2011; 32: 5706-5716.
29. Shahbazzadeh D, Ahari H, Motalebi AA, Anvar AA, Moaddab S, Asadi T, Shokrgozar MA, Rahman-Nya J. In vitro effect of Nanosilver toxicity on fibroblast and mesenchymal stem cell lines. *Iran J Fish Sci.* 2011; 10(3): 487-496.
30. Chang CJ, Hsu SH. The effect of high outflow permeability in asymmetric poly(DL-lactic acid-co-glycolic acid) conduits for peripheral nerve regeneration. *Biomaterials.* 2006; 27: 1035-1042.
31. Saravanan S, Nethala S, Pattnaik S, Tripathi A, Moorthi A, Selvamurugan N. Preparation, characterization and antimicrobial activity of abio-composite scaffold containing chitosan/nano-hydroxyapatite/nano-silver for bone tissue engineering. *Int J Biol Macromol.* 2011; 49: 188-193.

32. Tsai YC, Hsu PC, Lin YW, Wu TM. Silver nanoparticles in multiwalled carbon nano tube–Nafion for surface-enhanced Raman scattering chemical sensor. *Sensors and Actuators B*. 2009; 138: 5–8.
33. Li L, Li Y, Li J, Yao L. Antibacterial Properties of Nanosilver PLLA Fibrous Membranes. *J Nanomater*. 2009; 2009:1-5.
34. Park EJ, Yi J, Kim Y, Choi K, Park K. Silver nanoparticles induce cytotoxicity by a Trojan-horse type mechanism. *Toxicology in Vitro*. 2010; 24: 872–878.